

miR-5590-3p inhibits the proliferation and metastasis of renal cancer cells by targeting ROCK2 to inhibit proliferation, migration and invasion

QUELING LIU^{1,2}, ANYI ZHU³, WEIYIN GAO³, FU GUI⁴, YAN ZOU³,
XIAOCHENG ZHOU³ and ZHENG DONG HONG³

¹Department of Oncology; ²Key Laboratory of Clinical and Translational Cancer Research; Departments of ³Urology and ⁴Ophthalmology, The Second Affiliated Hospital of Nanchang University, Nanchang, Jiangxi 330006, P.R. China

Received September 7, 2021; Accepted February 22, 2022

DOI: 10.3892/ol.2022.13497

Abstract. The present study aimed to clarify the role of microRNA (miR)-5590-3p in the progression of renal cell carcinoma (RCC) and investigate the underlying mechanisms. The expression levels of miR-5590-3p, Rho-associated protein kinase (ROCK)2 and β -catenin in RCC cells were measured by reverse transcription-quantitative PCR and western blot analysis. Following overexpression of miR-5590-3p and ROCK2 by transfection of miR-5590-3p mimics and GV367-ROCK2, respectively, changes in the proliferation, migration and invasion of RCC cells were determined through colony-formation, wound-healing and Transwell assays, respectively. The direct binding interaction between miR-5590-3p and ROCK2, initially predicted using Targetscan, was validated by a dual-luciferase reporter assay. The results indicated that miR-5590-3p was downregulated in RCC. Overexpression of miR-5590-3p led to downregulation of ROCK2 and β -catenin and inhibited the proliferation, migration and invasion of RCC cells. The dual-luciferase reporter assay confirmed the binding relationship between miR-5590-3p and ROCK2. Of note, overexpression of ROCK2 effectively reversed the regulatory effects of miR-5590-3p on RCC cells. In conclusion, miR-5590-3p inhibits the proliferation, migration and invasion of RCC cells by targeting ROCK2, which is a potential molecular biomarker and therapeutic target for RCC.

Introduction

Renal cell carcinoma (RCC) originates from the renal tubular epithelium in the proximal convoluted tubule (1); it is the

14th most common cancer type in females and the 9th most common in males (2). The global incidence of RCC is ~4% and rises each year (3). The World Health Organization proposed that the annual number of RCC-associated deaths is as high as ~140,000 and it ranks 13th for cancer-associated mortality (4). The introduction of checkpoint inhibitor (CPI) therapy has led to a paradigm change in advanced RCC; dual immune checkpoint inhibition or the combination of CPI and tyrosine kinase inhibitors were indicated to improve survival (5). In addition, new data from trials of immune CPIs for advanced kidney cancer confirm a survival benefit with the combination of cabozantinib plus nivolumab, pembrolizumab plus axitinib and ipilimumab plus nivolumab (6). Although the diagnostic and therapeutic efficacies for treating RCC have been markedly improved during the past few decades, it remains one of the most lethal urinary system malignancies.

MicroRNAs (miRNAs/miRs) are a class of short non-coding RNAs that have been recognized as vital tumor regulators in recent years (7). Recent studies have indicated that miRNAs are involved in the regulation of multiple signaling pathways during the progression of RCC, serving in both oncogenic and tumor-suppressor roles. Therefore, miRNAs are thought to be potential therapeutic and prognostic targets in RCC (8). Maher (9) reviewed the changes in our understanding of the genetics of RCC, such as Hereditary BAP1-associated RCC (10) and activating mutations in the MET proto-oncogene predispose to Type 1 hereditary papillary RCC (11), while Huang *et al* (12) reported that miR-33b-5p may function as a tumor-suppressive regulator and prognostic biomarker in RCC progression and sunitinib resistance, which may provide novel therapeutic targets for sunitinib-resistant RCC. In recent years, the function of miR-5590-3p in mediating gene transcription in cancers, including breast cancer (13), prostate cancer (14) and gastric cancer (15), has been reported. Although the involvement of miR-5590-3p in RCC has been previously indicated (16), its regulatory mechanisms require further exploration.

Rho-associated protein kinase (ROCK) is a kinase belonging to the AGC family of serine-threonine kinases. The ROCK family consists of two isoforms, namely ROCK1 and ROCK2 (17). The ROCK signaling pathway has been well

Correspondence to: Professor Zhengdong Hong, Department of Urology, The Second Affiliated Hospital of Nanchang University, 1 Minde Road, Nanchang, Jiangxi 330006, P.R. China
E-mail: 3586273107@qq.com

Key words: renal cell carcinoma, miR-5590-3p, ROCK2, proliferation, migration, invasion

documented in various biological processes (18). Numerous studies have indicated that ROCK is associated with the accelerated metastasis of multiple types of tumors and reduced survival, which is expected from a cancer treatment target (19). It has been suggested that ROCK expression is negatively associated with the survival rate of patients with RCC. ROCK2 mediates RCC proliferation through the ROCK2/ β -catenin pathway (20). Therefore, ROCK is of great significance during the progression of RCC.

In the present study, it was predicted that miR-5590-3p directly targeted ROCK2 using Targetscan 7.1 and that this was abnormally expressed in clinical specimens and cell lines of RCC. It was then investigated how miR-5590-3p and ROCK2 regulated RCC cell functions and their exact molecular mechanism.

Materials and methods

Patients and samples. A total of six surgical RCC specimens were collected from patients with RCC who received surgery between January 1, 2018, and July 1, 2018, at the Second Affiliated Hospital of Nanchang University (Nanchang, China). Patients were not treated by any other means. This study was approved by the Second Affiliated Hospital of Nanchang University Medical Research Ethics Committee (Nanchang, China; no. 2017-100). Written informed consent was obtained from each participant prior to the study.

Cell culture. The RCC cell lines A498 (cat. no. BNCC350808) and A704 (cat. no. BNCC342393), the kidney fibroblast cell line KFB (cat. no. BNCC341253) and 293T human embryonic kidney cells (cat. no. BNCC100409) were purchased from BeNa Bio. and cultivated in DMEM containing 10% FBS (all from BeNa Bio.) and 1% penicillin and streptomycin in a humidified atmosphere with 5% CO₂ at 37°C.

Cell transfection. miR-5590-3p mimics and the negative control (NC) miR-5590-3p mimic-NC were provided by RiboBio Co., Ltd. (mimics sequence: 5'-AAUAAAGUUCAU GUAUGGCAA-3'; and mimic-NC sequence: 5'-UUCUCC GAACGUGUCACGUTT-3'). Cells were seeded in a 12-well plate (1x10⁵ cells/well) and cultivated to 80% confluence. After 4-h cell starvation in serum-free medium, cells were treated with a mixture containing 100 nM plasmid and Lipofectamine® 2000 reagent (Invitrogen; Thermo Fisher Scientific, Inc.) that was prepared at room temperature 20 min previously. After 24 h of incubation, the culture supernatant was replaced with fresh medium and the mimics expression efficacy was examined by reverse transcription-quantitative (RT-q)PCR.

RT-qPCR. Total RNA was isolated from RCC cells using TRIzol Reagent (Invitrogen; Thermo Fisher Scientific, Inc.) and cDNA was obtained through RT using the Primescript™ RT reagent kit with gDNA Eraser (Takara Bio, Inc.) according to the manufacturer's protocol. SYBR Premix Ex Taq™ II (Tli RNaseH Plus; Takara Bio, Inc.) was used in a fluorescence quantitative PCR system (Bio-Rad, Inc.) to perform qPCR, using 0.2 μ l of cDNA as the template and the following thermocycling program: 95°C for 30 sec, followed by 40 cycles at 95°C for 10 sec and 60°C for 30 sec, and finally extension

at 60°C for 10 min. The relative expression level was calculated using the 2^{- $\Delta\Delta$ Cq} method (21). GAPDH or U6 served as the internal reference. The primer sequences are listed in Table I.

Western blot analysis. Total protein was isolated using RIPA buffer (Beyotime Institute of Biotechnology, Inc.) and quantified using the BCA method. The protein sample (50 μ g per lane) was separated on 10% gels using SDS-PAGE, transferred onto PVDF membranes (MilliporeSigma) and immersed in Tris-buffered saline with Tween-20 containing 5% skimmed milk (Sangon Biotech, Inc.). After immunoblotting with primary antibodies (1:1,000 dilution) at 4°C overnight and secondary antibodies (1:1,000 dilution) at room temperature for 1 h. ECL luminescence reagent (Sangon Biotech, Co., Ltd.) was added dropwise onto the PVDF membrane. Bands were visualized using the Bio-Rad Universal Hood II Gel Doc Imaging system (Bio-Rad Laboratories, Inc.) and grey values were analyzed using Image J software version 1.8.0.112 [US National Institutes of Health (NIH)]. All antibodies used were purchased from Abclonal as follows: ROCK2 (cat. no. A2395); β -catenin (cat. no. A19657); AKT (cat. no. A17909); MMP-2 (cat. no. A19080); GAPDH (cat. no. A19056); and the secondary antibody (cat. no. AS014).

Lentivirus transfection. Target gene fragments were designed and synthesized based on gene sequences retrieved from GenBank and a lentiviral recombinant overexpression plasmid was synthesized. The overexpression plasmid and the empty plasmid were GV367-ROCK2 and GV367 (GeneChem, Inc.), respectively. The lentiviral plasmid, packaging vector and envelope vector (GeneChem, Inc.) were mixed at 4:3:2, with a total DNA mass of 20 μ g. The mixture was incubated with 1 ml of Lenti-Easy Packaging Mix (Shanghai GeneChem Co., Ltd.) for 15 min and Lipofectamine® 2000 for 20 min. Subsequently, they were added to the culture medium of 293T cells for 6 h at 37°C; the medium was replaced with fresh medium after 6 h of incubation to continue the culture. Three days later, the 293T cells were filtered using a 0.45- μ M mesh, centrifuged at 70,000 x g at 4°C for 2 h and the supernatant was collected for detecting viral titers. RCC cells with 80% of confluence were cultured with diluted lentiviruses and green fluorescence protein-labeled cells with a minimum lentivirus transfection rate of 80% at 72 h were screened. The overexpression efficacy was verified by RT-qPCR.

Colony formation assay. Cells were seeded in a six-well plate (5x10² cells/well) with 37°C. Cell culture was terminated when the majority of visible colonies contained >50 cells and they were then fixed with 4% paraformaldehyde at room temperature for 20 min and stained using 0.2% crystal violet at room temperature for 10 min. After washing, images of each well were captured for calculating the number of colonies in three replicates per sample.

Wound-healing assay. Cells were seeded in a 12-well plate (1x10⁵ cells/well) and cultivated in serum-free medium for 12 h. A sterile pipette tip was used to create an artificial wound in the cell monolayer and cell migration at 24 h was assessed by calculating the cell-free zone at 24 vs. 0 h using Image J software version 1.8.0.112 (NIH).

Table I. PCR primers used in the present study.

Gene	Primer (5'-3')
miR-5590-3p-F	ACACTCCAGCTGGGAATAAAGTTCATGTA
miR-5590-3p-R	CTCAACTGGTGTCTCGTGGAGTCGGCAATTCAGTTGAGTTGCCATA
ROCK2-F	TCAGAGGTCTACAGATGAAGGC
ROCK2-R	CCAGGGGCTATTGGCAAAGG
β -catenin-F	AGCTTCCAGACACGCTATCAT
β -catenin-R	CGGTACAACGAGCTGTTTCTAC
AKT-F	GAAGCTGAGCCCACCTTCA
AKT-R	CATCTTGATCAGGCGGTGTG
MMP2-F	TGATCTTGACCAGAATACCATCGA
MMP2-R	GGCTTGCGAGGGAAGAAGTT
GAPDH-F	AATCCCATCACCATCTTCCAG
GAPDH-R	GAGCCCCAGCCTTCTCCAT
U6-F	GCTTCGGCAGCACATATACTAAAAT
U6-R	CGCTTCACGAATTTGCGTGTTCAT

ROCK, Rho-associated protein kinase; F, forward; R, reverse; miR, microRNA.

Transwell assay. Cells (5×10^4 cells) were seeded in the upper chambers of a Transwell insert (8 μ m pore size; BD Biosciences, Inc.) pre-coated with Matrigel[®] and 700 μ l of DMEM containing 10% FBS and 1% penicillin and streptomycin was added to the bottom wells. After 24 h of cell culture, cells were stained using crystal violet at 37°C for 5 min. After being washed and air-dried, invaded cells were calculated in five randomly selected fields per well.

Dual-luciferase reporter assay. Target prediction for ROCK2 3'-UTR and miR-5590-3p was performed using TargetScan 7.2 (http://www.TargetScan.org/vert_72/). Complementary sequences in the ROCK2 3'-UTR and miR-5590-3p promoter region were cloned into the 3'-UTR of pGL3 (Genechem, Inc.) to construct the wild-type plasmid, pGL3-ROCK2-wt, and the mutant-type plasmid, pGL3-ROCK2-mut, was generated using the GeneTailer site-directed mutagenesis kit (Invitrogen; Thermo Fisher Scientific, Inc.). They were co-transfected into cells with miR-5590-3p mimics or miR-5590-3p mimic-NC in a 96-well plate for 48 h. Luciferase activities were measured using the Dual-Luciferase Reporter Gene Assay Kit (Promega Corporation).

Immunohistochemical detection. The RCC sections were incubated in xylene (15 min, three times), dehydrated in anhydrous ethanol (5 min, twice), 85% ethanol (5 min, once) and 75% ethanol (5 min, once), and washed in ddH₂O. Antigen retrieval was performed by pouring citrate buffer (pH 6.0; Sangon Biotech, Co., Ltd.; cat. no. E673000) on the sections for 15 min. After incubation in 3% H₂O₂ in the dark for 25 min and blocking with 3% BSA (Sangon Biotech, Co., Ltd.; cat. no. E661003) at 37°C for 30 min, the sections were incubated with primary antibodies against ROCK2 diluted at 1:50 (cat. no. A2395; Abclonal, Inc.) at 4°C overnight. Next, the sections were washed in PBS (pH 7.4, 5 min, three times) and incubated with HRP-labeled secondary antibody diluted

at 1:500 (cat. no. AS002; Abclonal, Inc.) at room temperature for 2 h. The sections were then counterstained with DAB and hematoxylin for 3 min. After dehydration in ddH₂O, 75% ethanol (5 min, once), 85% ethanol (5 min, once), anhydrous ethanol (5 min, twice) and *n*-butanol (5 min, once) sequentially, and permeabilization in xylene (5 min, once), neutral gum was used for mounting. The positive staining of cells was observed under a microscope (XSP-8CA; Shanghai Optical Instrument Co., Ltd.).

Statistical analysis. GraphPad Prism 8.0 (GraphPad Software, Inc.) was used for statistical analyses. Values are expressed as the mean \pm standard deviation. All data conformed to a normal distribution. In the cell experiment, comparisons between two groups were performed using the unpaired t-test, while for comparisons among multiple groups, one-way analysis of variance followed by Tukey's or Bonferroni's post-hoc test were used. For the data comparison of tumor tissues, a paired t-test was used. The correlation analysis was performed by Spearman's correlation test. $P < 0.05$ was considered to indicate statistical significance. Each experiment was performed in triplicate.

Results

Aberrant expression of miR-5590-3p and ROCK2 in RCC samples and cell lines. RCC samples and paracancerous tissues (~4 cm from the edge of the cancer and confirmed as non-cancerous by histological examination) were collected from 6 cases of RCC (4 male and 2 female patients; age range, 47-55 years old) for isolating total RNA and protein (Table II). The analyses indicated that miR-5590-3p was significantly downregulated (Fig. 1A). By contrast, ROCK2 was upregulated in RCC samples compared to adjacent controls both at the mRNA and protein levels (Fig. 1B and C). Immunohistochemical detection of ROCK2 expression in

Table II. Patient information.

Case no.	Age, years	Sex	Stage ^a
1	47	Male	T2N0M0, II
2	48	Male	T2N2cM0, IVb
3	52	Male	T3N2bM0, IVb
4	55	Male	T3N2bM0, IVb
5	51	Female	T2N2cM0, IVb
6	54	Female	T3N2bM0, IVb

^a(37).

tumor and adjacent tissues provided similar results (Fig. 1D). Furthermore, the expression of miR-5590-3p and ROCK2 exhibited a significant negative correlation (Fig. 1E). Downregulated miR-5590-3p and upregulated ROCK2 were also detected in RCC cell lines (Fig. 1F-H). Those results suggested that miR-5590-3p and ROCK2 are abnormally expressed in RCC.

miR-5590-3p targets and downregulates ROCK2. As predicted by Targetscan 7.1, complementary binding sites were present in the miR-5590-3p promoter region and ROCK2 3'-UTR (Fig. 2A). Subsequently, luciferase activity in cells co-transfected with pcDNA3.1-ROCK2-wt and miR-5590-3p mimics was only 51.33 and 42.68% of that in those co-transfected with pcDNA3.1-ROCK2-wt and miR-5590-3p mimics-NC. Overexpression of miR-5590-3p, however, did not significantly change the luciferase reporter activity in cells transfected with pcDNA3.1-ROCK2-mut (Fig. 2B). In RCC cells overexpressing miR-5590-3p, the mRNA and protein levels of ROCK2 were both downregulated (Fig. 2C-E). This suggests that miR-5590-3p directly targets and downregulates ROCK2 in RCC cell lines.

miR-5590-3p suppresses the proliferative, migratory and invasive capacities of RCC cells. After transfection of miR-5590-3p mimics for 48 h, cells were collected to examine the overexpression efficacy by RT-qPCR (Fig. 3A). Compared with those transfected with NC, RCC cells transfected with miR-5590-3p mimics had reduced proliferative (Fig. 3B), migratory (Fig. 3C) and invasive capacities (Fig. 3D). In addition, the mRNA and protein levels of ROCK2 and β -catenin were significantly downregulated in RCC cell lines overexpressing miR-5590-3p. Genes associated with cell proliferation, migration and invasion, were also examined and it was indicated that AKT and MMP-2 were also significantly downregulated (Fig. 3E and F). Collectively, overexpression of miR-5590-3p significantly downregulated β -catenin, AKT and MMP-2, and suppressed the proliferation and metastasis of RCC cells.

Overexpression of ROCK2 promotes the proliferative, migratory and invasive capacities of RCC cells and reverses the regulatory effects of miR-5590-3p. The overexpression efficacy of the lentivirus GV367-ROCK2 was examined first (Fig. 4A), followed by examination of ROCK2 and

miR-5590-3p levels in RCC cells co-transfected with GV367-ROCK2 and miR-5590-3p mimics (Fig. 4B). Of note, overexpression of ROCK2 significantly stimulated the proliferative, migratory and invasive capacities of RCC cells, and it reversed the inhibitory effects of miR-5590-3p on the above-mentioned cell behaviors (Fig. 4C-E). Furthermore, β -catenin, AKT and MMP-2 were upregulated in RCC cells overexpressing ROCK2 (Fig. 4F and G). Therefore, it was indicated that miR-5590-3p downregulated β -catenin, AKT and MMP-2, and inhibited the proliferation and metastasis of RCC cells through targeting ROCK2.

Discussion

RCC is the most common malignant tumor type of the urinary system. RCC may be classified by pathological subtype, among which clear cell renal cell carcinoma (ccRCC) is the most prevalent, accounting for 75-80% of RCC cases (22). Approximately 30% of patients with ccRCC develop metastatic RCC after curative nephrectomy (23) and are the high-risk population for RCC-associated death (24). The morbidity and mortality of advanced RCC are high and the five-year survival is only 18% (25). Although surgical resection, chemotherapy and radiotherapy are preferred treatments for patients with RCC, their therapeutic efficacies are far away from satisfying. Thus, it is of great significance to seek novel biomarkers in order to facilitate early diagnosis and improve the prognosis of RCC.

miRNAs are highly conserved endogenous RNAs. Following a series of complex biological processes, miRNAs form the RNA-induced silencing complex and bind to the target gene's 3'-UTR to regulate their post-transcriptional levels (26). miRNAs are highly associated with tumor cell functions, including proliferation, apoptosis and migration. The role of miRNAs in the progression of RCC has been previously reported. Çaykara *et al* (27) indicated that abnormally downregulated miR-124 was associated with the tumor stage, tumor size and neutrophil count in patients with RCC, and restoration of miR-124 expression may be effective in the treatment of RCC. He *et al* (28) reported that miR-125b was significantly upregulated in RCC tissues, which was negatively correlated with vitamin D receptor (VDR) levels. Through mediating VDR, miR-125 is capable of enhancing proliferative and migratory rates of RCC cells, suggesting miR-125 may be a potential therapeutic target of RCC. Chen *et al* (29) determined that miR-26a-5p is lowly expressed in RCC samples. Overexpression of miR-26a-5p inhibited the migration, invasion and metastasis of RCC, and induced apoptosis of RCC cells by targeting E2F7. miR-5590-3p is a recently discovered miRNA exerting important functions in tumor signaling. Zhang *et al* (30) reported that miR-5590-3p exerts a sponge effect on SOX9-antisense 1 (AS1) and thus upregulates SOX9, and the activated downstream Wnt/ β -catenin signaling pathway drives the growth and metastasis of hepatocellular carcinoma through triggering epithelial-mesenchymal transition (EMT). Wu *et al* (15) compared miR-5590-3p levels in gastric cancer tissues with adjacent normal tissues and determined that it is significantly downregulated in the former. They additionally validated that miR-5590-3p inhibits gastric cancer growth by directly targeting DEAD-box helicase 5 in an *in vivo*

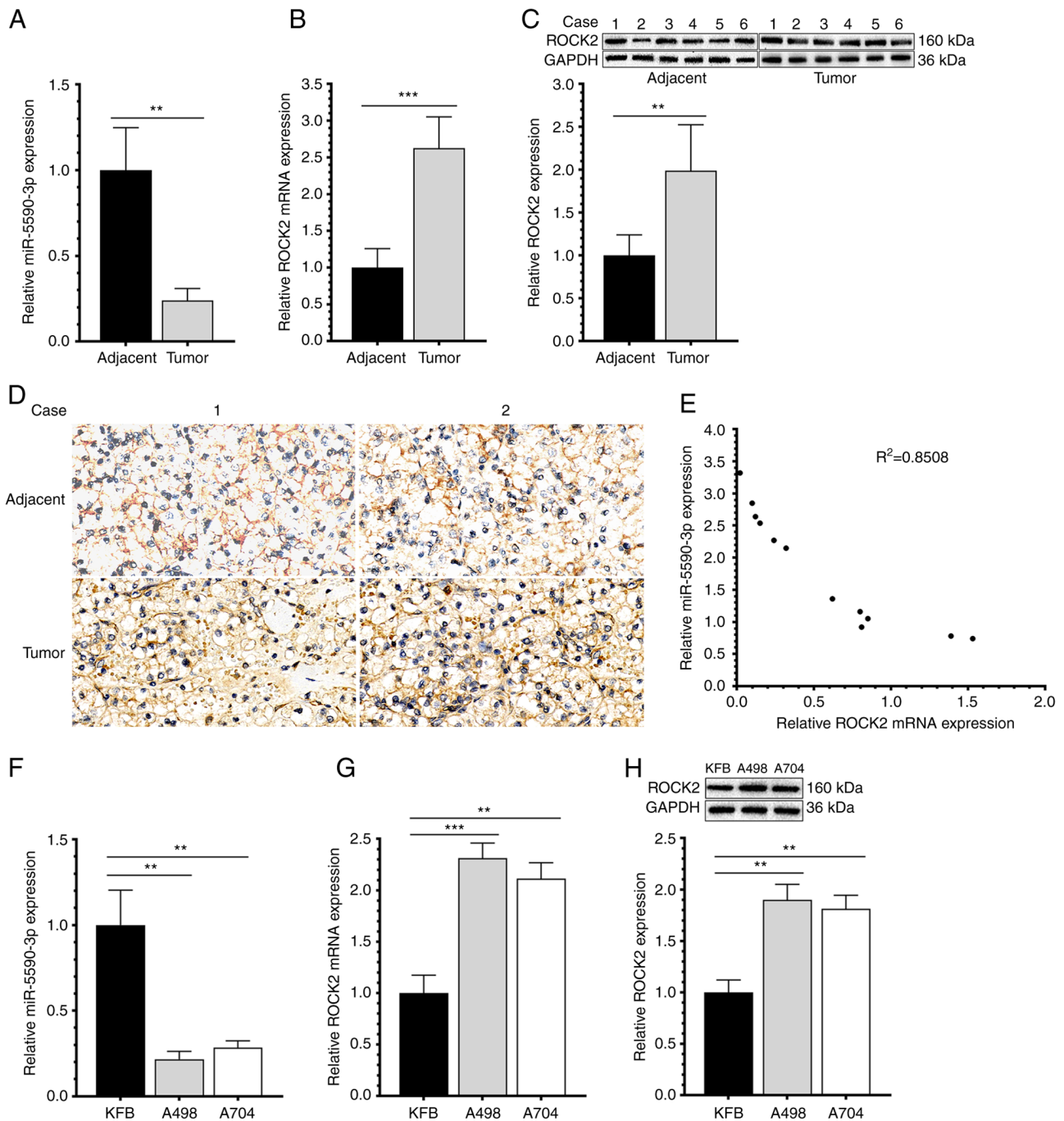


Figure 1. Aberrant expression of miR-5590-3p and ROCK2 in patients with RCC and in RCC cell lines. (A) Relative miR-5590-3p expression in patients with RCC; (B) relative ROCK2 mRNA expression in patients with RCC; (C) relative ROCK2 protein expression in patients with RCC (cases 1-6); (D) immunohistochemical analysis of ROCK2 expression in patients with RCC (case 1 and 2) (magnification, x100); (E) correlation between miR-5590-3p and ROCK2 expression in the tumor and adjacent tissues; (F) relative miR-5590-3p expression in RCC cell lines; (G) relative ROCK2 mRNA expression in RCC cell lines; (H) relative ROCK2 protein expression in RCC cell lines. ** $P < 0.01$; *** $P < 0.001$. ROCK, Rho-associated protein kinase; miR, microRNA; RCC, renal cell carcinoma.

xenograft nude mouse model, as well as in gastric cancer cell line models *in vitro*. Yang *et al* (31) demonstrated that lncRNA FYVE, RhoGEF and PH domain containing 5-AS1 competitively interacts with miR-5590-3p, thereby mediating ccRCC cell proliferation and metastasis by activating ERK/AKT signaling. In the present study, miR-5590-3p was significantly downregulated in RCC samples compared with that in normal tissues, and as expected, it was lowly expressed in RCC cell lines. Transfection of miR-5590-3p mimics effectively

inhibited the proliferative, migratory and invasive capacities of RCC cells, and downregulated the mRNA and protein levels of β -catenin, AKT and MMP-2. It was concluded that miR-5590-3p was important in the progression of RCC and its overexpression effectively inhibited the proliferation and metastasis of RCC cells.

ROCK2 is the downstream effector of the Rho family of GTPases, which is responsible for mediating gene expression by regulating their activities or phosphorylation (32). ROCK2

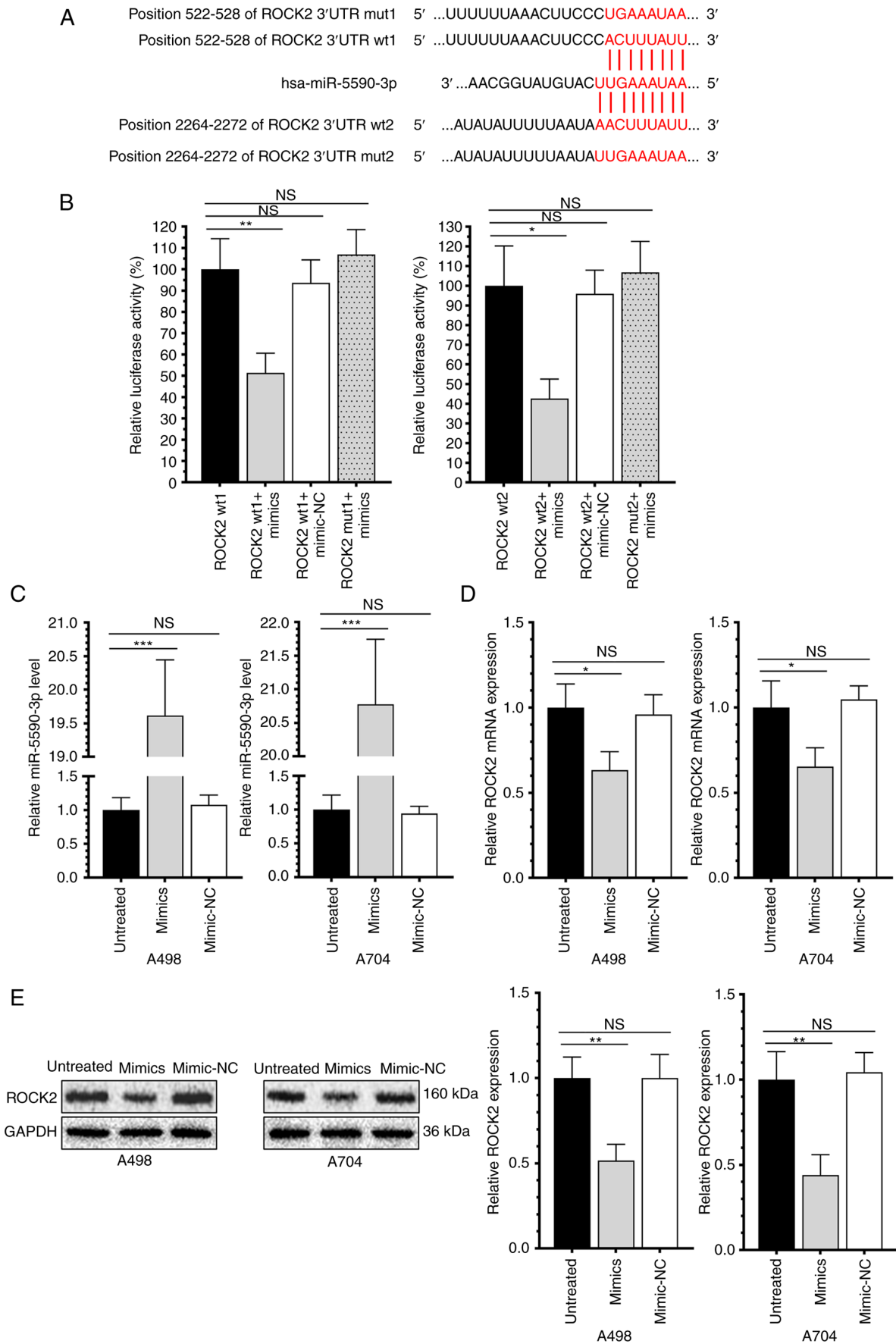


Figure 2. miR-5590-3p directly targets ROCK2 and downregulates its expression. (A) Prediction of the targeting relationship between miR-5590-3p and ROCK2; (B) dual-luciferase reporter assay to confirm the interaction between miR-5590-3p and ROCK2; (C) expression efficiency of miR-5590-3p mimics and NC; (D) relative ROCK2 mRNA expression in RCC cells transfected with miR-5590-3p mimics or NC; (E) relative ROCK2 protein expression of RCC cells transfected with miR-5590-3p mimics or NC. * $P < 0.05$; ** $P < 0.01$; *** $P < 0.001$. NS, no significance; ROCK, Rho-associated protein kinase; miR, microRNA; RCC, renal cell carcinoma; wt, wild-type; mut, mutant; NC, negative control.

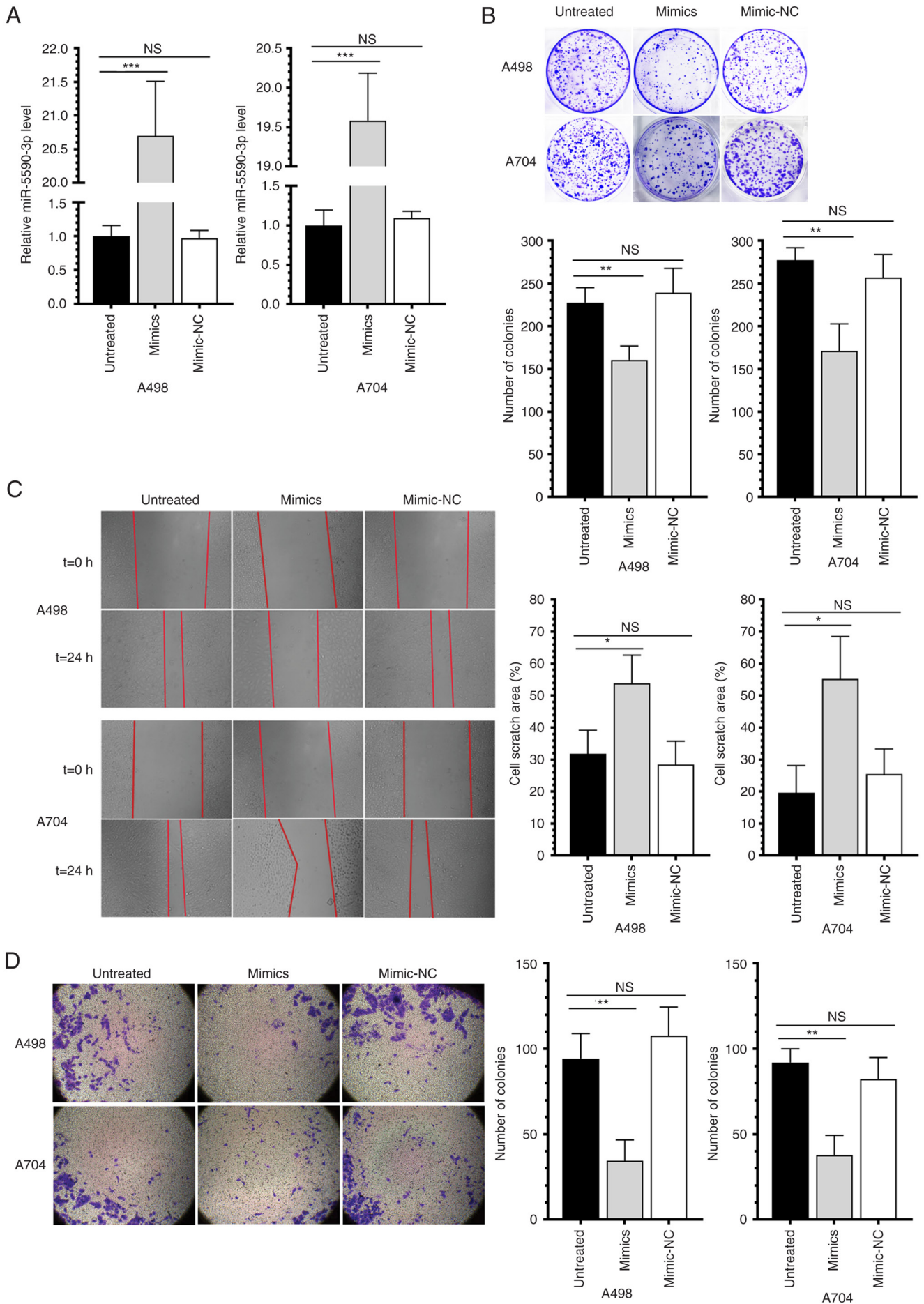


Figure 3. Continued.

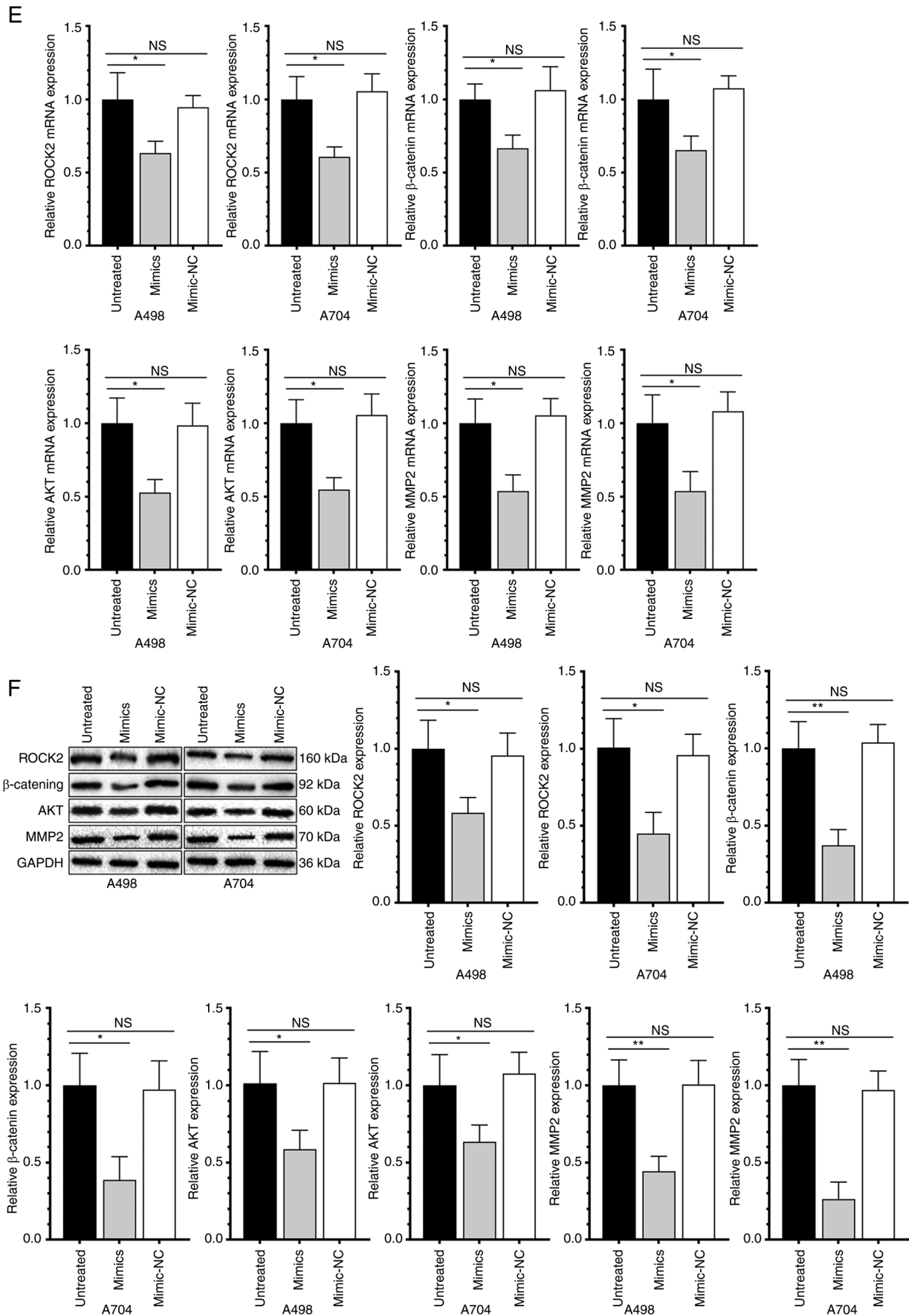


Figure 3. miR-5590-3p significantly inhibits RCC. (A) Transfection efficiency of miR-5590-3p mimics and NC; (B) cell proliferation ability of RCC cell lines transfected with miR-5590-3p mimics or NC; (C) cell migration ability of RCC cell lines transfected with miR-5590-3p mimics or NC (magnification, x100); (D) cell invasion ability of RCC cell lines transfected with miR-5590-3p mimics or NC; (E) mRNA expression of key genes in RCC cell lines transfected with miR-5590-3p mimics or NC (magnification, x100); (F) protein expression of key genes in RCC cell lines transfected with miR-5590-3p mimics or NC. *P<0.05; **P<0.01; ***P<0.001. NS, no significance; NC, negative control; miR, microRNA; RCC, renal cell carcinoma; ROCK, Rho-associated protein kinase.

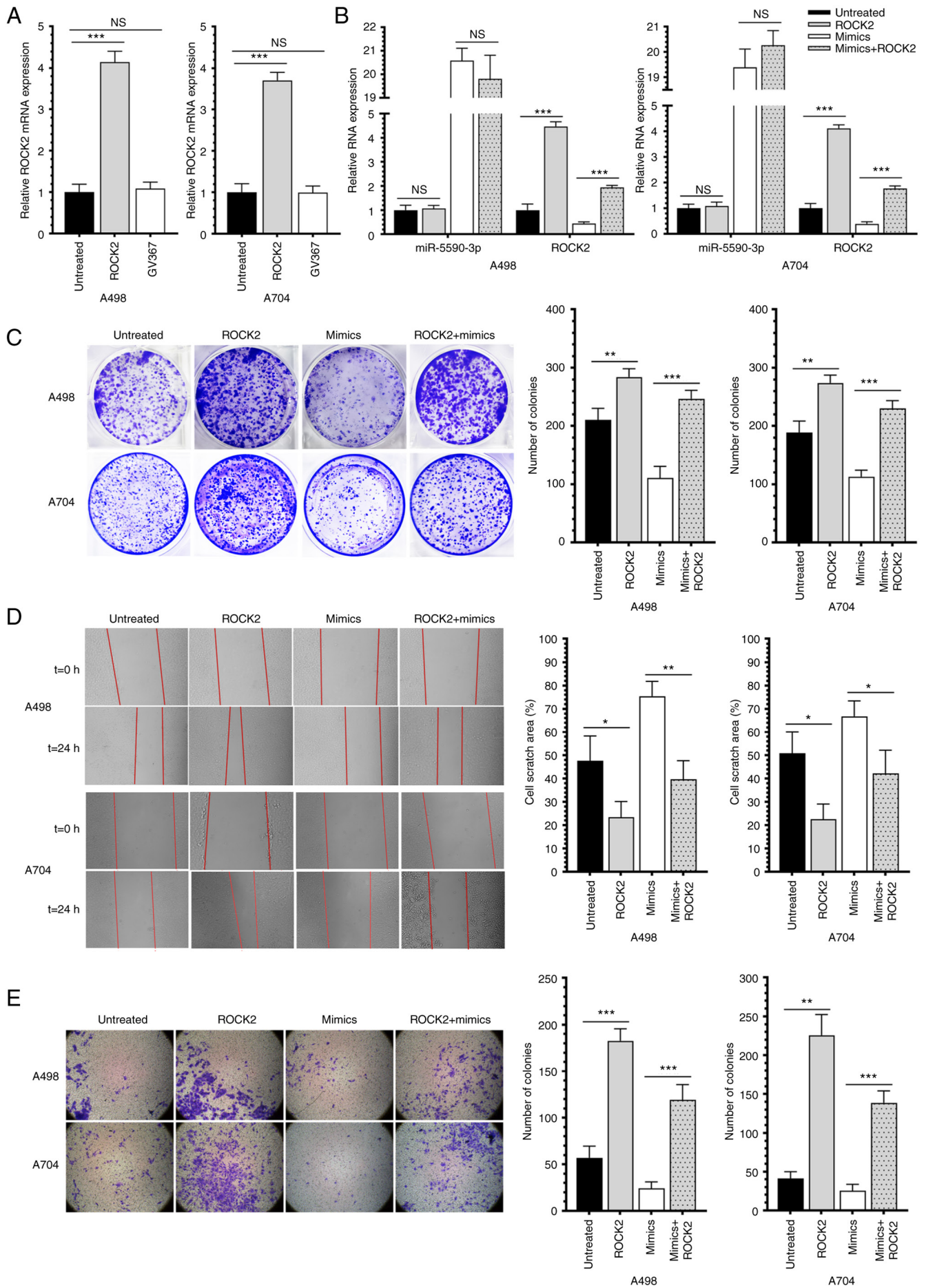


Figure 4. Continued.

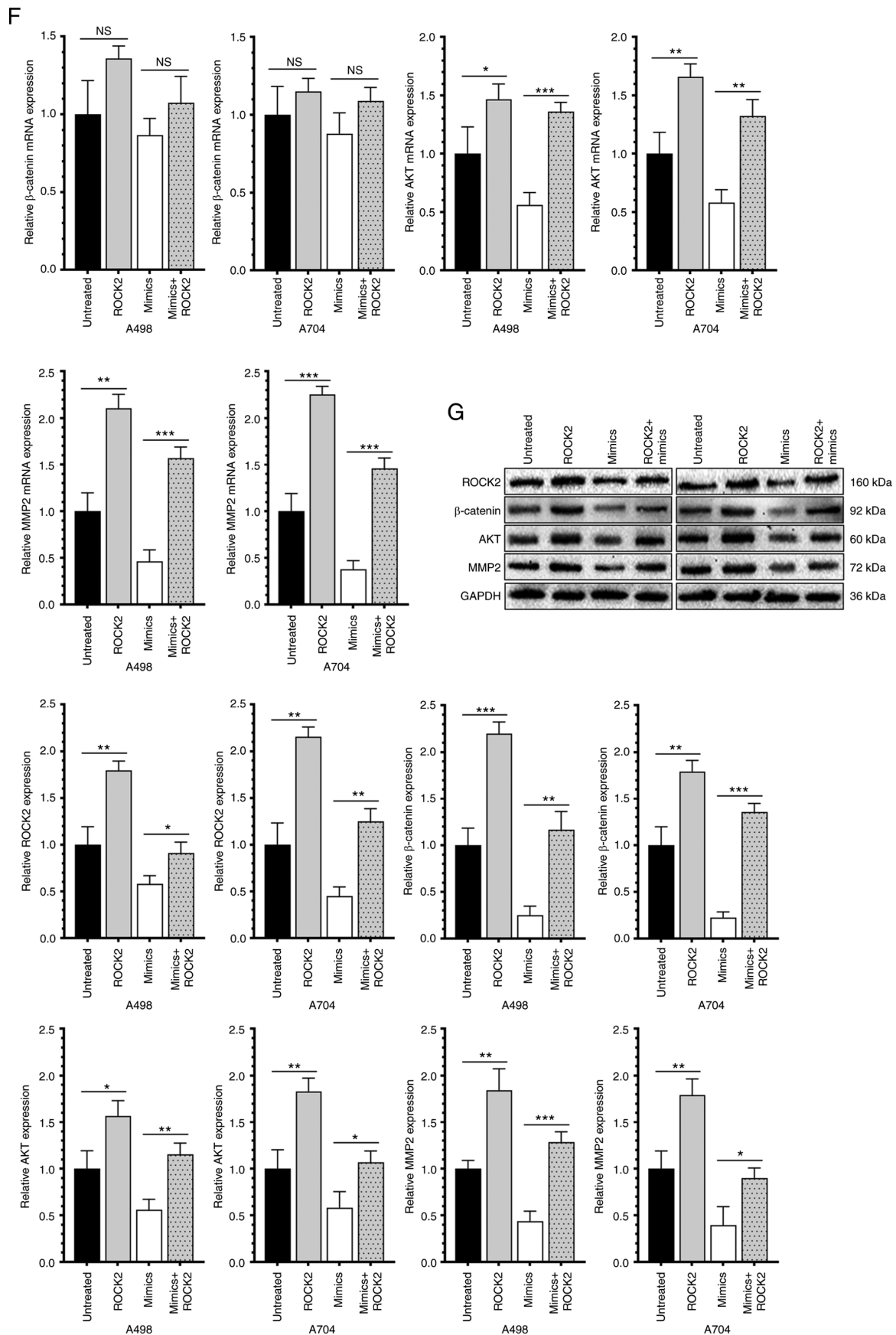


Figure 4. ROCK2 promotes RCC and reverses the effect of miR-5590-3p. (A) Overexpression efficiency following lentivirus transfection; (B) co-transfection efficiency of miR-5590-3p and ROCK2; (C) cell proliferation ability of RCC cell lines co-transfected with miR-5590-3p and ROCK2; (D) cell invasion ability of RCC cell lines co-transfected with miR-5590-3p and ROCK2 (magnification, x100); (E) cell invasion ability of RCC cell lines co-transfected with miR-5590-3p and ROCK2 (magnification, x100); (F) mRNA expression of key genes in RCC cell lines co-transfected with miR-5590-3p and ROCK2; (G) protein expression of key genes in RCC cell lines co-transfected with miR-5590-3p and ROCK2. * $P < 0.05$; ** $P < 0.01$; *** $P < 0.001$. NS, no significance; ROCK, Rho-associated protein kinase; miR, microRNA; RCC, renal cell carcinoma.

is closely linked with tumorigenesis and tumor development by influencing cancer cell functions (33), and as a result, it has become a well-studied target for designing novel anti-cancer drugs. Multiple studies have detected high expression of ROCK2 in cancer tissues. Deng *et al* (34) reported that ROCK2 was upregulated in osteosarcoma tissues compared to those of adjacent ones, and it stimulated the malignant growth of osteosarcoma by upregulating HKII through phosphorylating the PI3K/AKT signaling pathway. Luo *et al* (35) discovered that ROCK2 was upregulated in the bladder cancer cell line T24 under hypoxic conditions. It inhibited apoptosis and induced proliferation, migration, invasion and EMT by activating the Wnt signaling pathway. Compared with non-cancerous tissues, Qiu *et al* (36) detected a higher level of ROCK2 in colorectal cancer (CRC) tissues; the high level of ROCK2 was significantly associated with metastasis and poor prognosis of CRC. ROCK2 stabilizes β -catenin by preventing its ubiquitination, thereby stimulating metastasis of RCC cells. Xu *et al* (20) revealed that ROCK2 is significantly upregulated in clinical samples of RCC. ROCK2 promotes RCC proliferation by decreasing scavenger receptor class A member 5 expression through β -catenin/transcription factor 4 signaling. The present study also consistently detected the upregulation of ROCK2 at both the mRNA and protein levels in RCC cells. It was indicated that ROCK2 was significant to the progression of RCC and may be regulated by miR-5590-3p.

Next, the targeting relationship between miR-5590-3p and ROCK2 was investigated. Through target sequence prediction using Targetscan 7.1 and validation by a dual-luciferase reporter assay, miR-5590-3p was confirmed to bind to the 3'-UTR of ROCK2. Overexpression of miR-5590-3p significantly downregulated the mRNA and protein levels of ROCK2, suggesting that miR-5590-3p targeted and downregulated ROCK2, which was able to further downregulate the expression of β -catenin, AKT and MMP-2. GV367-ROCK2 was subsequently transfected into RCC cells, resulting in enhanced proliferative and metastatic capacities. Furthermore, overexpression of ROCK2 significantly promoted the proliferation, migration and invasion of RCC cells, and, of note, reversed the inhibitory effects of miR-5590-3p on the malignant behaviors of RCC cells. It was concluded that miR-5590-3p directly targeted ROCK2 and this led to a decrease in the expression of β -catenin, AKT and MMP-2, thereby inhibiting the proliferation and metastasis of RCC.

In conclusion, miR-5590-3p inhibits the proliferation, migration and invasion of RCC cells by targeting ROCK2, which is a potential molecular biomarker and therapeutic target of RCC.

Acknowledgements

Not applicable.

Funding

This project was funded by the National Natural Science Foundation of China (grant no. 81760458).

Availability of data and materials

The datasets used and analyzed during the current study are available from the corresponding author on reasonable request.

Authors' contributions

QL, ZH and AZ contributed to the study conception and design, and the acquisition of data. WG, ZH, YZ, XZ and FG contributed to the analysis and interpretation of the data. QL and ZH confirm the authenticity of all the raw data. All authors contributed to the writing of the article and have read and approved the manuscript.

Ethics approval and consent to participate

This study was approved by the Second Affiliated Hospital of Nanchang University Medical Research Ethics Committee (Nanchang, China; approval no. 2017-100). Written informed consent was obtained from each participant prior to the study.

Patient consent for publication

Not applicable.

Competing interests

The authors declare that they have no competing interests.

References

1. Koul H, Huh JS, Rove KO, Crompton L, Koul S, Meacham RB and Kim FJ: Molecular aspects of renal cell carcinoma: A review. *Am J Cancer Res* 1: 240-254, 2011.
2. Bray F, Ferlay J, Soerjomataram I, Siegel RL, Torre LA and Jemal A: Global cancer statistics 2018: GLOBOCAN estimates of incidence and mortality worldwide for 36 cancers in 185 countries. *CA Cancer J Clin* 68: 394-424, 2018.
3. Ahrens M, Scheich S, Hartmann A and Bergmann L; IAG-N Interdisciplinary Working Group Kidney Cancer of the German Cancer Society: Non-clear cell renal cell carcinoma-pathology and treatment options. *Oncol Res Treat* 42: 128-135, 2019.
4. Capitanio U, Bensalah K, Bex A, Boorjian SA, Bray F, Coleman J, Gore JL, Sun M, Wood C and Russo P: Epidemiology of Renal Cell Carcinoma. *Eur Urol* 75: 74-84, 2019.
5. Bruchbacher A, Lemberger U, Hassler MR, Fajkovic H and Schmidinger M: PD1/PD-L1 therapy in metastatic renal cell carcinoma. *Curr Opin Urol* 30: 534-541, 2020.
6. Bedke J, Albiges L, Capitanio U, Giles RH, Hora M, Lam TB, Ljungberg B, Marconi L, Klatt T, Volpe A, *et al*: Updated European Association of Urology guidelines on renal cell carcinoma: Nivolumab plus cabozantinib joins immune checkpoint inhibition combination Therapies for treatment-naive metastatic clear-cell renal cell carcinoma. *Eur Urol* 79: 339-342, 2021.
7. Rupaimoole R and Slack FJ: MicroRNA therapeutics: Towards a new era for the management of cancer and other diseases. *Nat Rev Drug Discov* 16: 203-222, 2017.
8. Yang L, Zou X, Zou J and Zhang G: A review of recent research on the role of MicroRNAs in renal cancer. *Med Sci Monit* 27: e930639, 2021.
9. Maher ER: Hereditary renal cell carcinoma syndromes: Diagnosis, surveillance and management. *World J Urol* 36: 1891-1898, 2018.
10. Testa JR, Cheung M, Pei J, Below JE, Tan Y, Sementino E, Cox NJ, Dogan AU, Pass HI, Trusa S, *et al*: Germline BAP1 mutations predispose to malignant mesothelioma. *Nat Genet* 43: 1022-1025, 2011.
11. Schmidt L, Duh FM, Chen F, Kishida T, Glenn G, Choyke P, Scherer SW, Zhuang Z, Lubensky I, Dean M, *et al*: Germline and somatic mutations in the tyrosine kinase domain of the MET proto-oncogene in papillary renal carcinomas. *Nat Genet* 16: 68-73, 1997.
12. Huang G, Lai Y, Pan X, Zhou L, Quan J, Zhao L, Li Z, Lin C, Wang J, Li H, *et al*: Tumor suppressor miR-33b-5p regulates cellular function and acts a prognostic biomarker in RCC. *Am J Transl Res* 12: 3346-3360, 2020.

13. Chen FY, Zhou ZY, Zhang KJ, Pang J and Wang SM: Long non-coding RNA MIR100HG promotes the migration, invasion and proliferation of triple-negative breast cancer cells by targeting the miR-5590-3p/OTX1 axis. *Cancer Cell Int* 20: 508, 2020.
14. Luo ZF, Peng Y, Liu FH, Ma JS, Hu G, Lai SL, Lin H, Chen JJ, Zou GM, Yan Q and Sui WG: Long noncoding RNA SNHG14 promotes malignancy of prostate cancer by regulating with miR-5590-3p/Y1 axis. *Eur Rev Med Pharmacol Sci* 24: 4697-4709, 2020.
15. Wu N, Han Y, Liu H, Jiang M, Chu Y, Cao J, Lin J, Liu Y, Xu B and Xie X: MiR-5590-3p inhibited tumor growth in gastric cancer by targeting DDX5/AKT/m-TOR pathway. *Biochem Biophys Res Commun* 503: 1491-1497, 2018.
16. Yang Y, Dong MH, Hu HM, Min QH and Xiao L: LncRNA FGD5-AS1/miR-5590-3p axis facilitates the proliferation and metastasis of renal cell carcinoma through ERK/AKT signalling. *Eur Rev Med Pharmacol Sci* 24: 8756-8766, 2020.
17. Sharma P and Roy K: ROCK-2-selective targeting and its therapeutic outcomes. *Drug Discov Today* 25: 446-455, 2020.
18. Wei L, Surma M, Shi S, Lambert-Cheatham N and Shi J: Novel insights into the roles of rho kinase in cancer. *Arch Immunol Ther Exp (Warsz)* 64: 259-278, 2016.
19. de Sousa GR, Vieira GM, das Chagas PF, Pezuk JA and Brassesco MS: Should we keep rocking? Portraits from targeting Rho kinases in cancer. *Pharmacol Res* 160: 105093, 2020.
20. Xu Z, Hong Z, Ma M, Liu X, Chen L, Zheng C, Xi X and Shao J: Rock2 promotes RCC proliferation by decreasing SCARA5 expression through β -catenin/TCF4 signaling. *Biochem Biophys Res Commun* 480: 586-593, 2016.
21. Livak KJ and Schmittgen TD: Analysis of relative gene expression data using real-time quantitative PCR and the 2(-Delta Delta C(T)) Method. *Methods* 25: 402-408, 2001.
22. Marchetti A, Rosellini M, Mollica V, Rizzo A, Tassinari E, Nuvola G, Cimadamore A, Santoni M, Fiorentino M, Montironi R and Massari F: The molecular characteristics of non-clear cell renal cell carcinoma: What's the story morning glory? *Int J Mol Sci* 22: 6237, 2021.
23. Sharma R, Kadife E, Myers M, Kannourakis G, Prithviraj P and Ahmed N: Determinants of resistance to VEGF-TKI and immune checkpoint inhibitors in metastatic renal cell carcinoma. *J Exp Clin Cancer Res* 40: 186, 2021.
24. Mlcochova H, Machackova T, Rabiien A, Radova L, Fabian P, Iliev R, Slaba K, Poprach A, Kilic E, Stanik M, *et al*: Epithelial-mesenchymal transition-associated microRNA/mRNA signature is linked to metastasis and prognosis in clear-cell renal cell carcinoma. *Sci Rep* 6: 31852, 2016.
25. Bhat S: Role of surgery in advanced/metastatic renal cell carcinoma. *Indian J Urol* 26: 167-176, 2010.
26. Winter J, Jung S, Keller S, Gregory RI and Diederichs S: Many roads to maturity: MicroRNA biogenesis pathways and their regulation. *Nat Cell Biol* 11: 228-234, 2009.
27. Caykara B, Ozturk G, Alsaadoni H, Otunctemur A and Pence S: Evaluation of MicroRNA-124 expression in renal cell carcinoma. *Balkan J Med Genet* 23: 73-78, 2021.
28. He X, Liao S, Lu D, Zhang F, Sun Y and Wu Y: MiR-125b promotes migration and invasion by targeting the vitamin D receptor in renal cell carcinoma. *Int J Med Sci* 18: 150-156, 2021.
29. Cheng C, Guo L, Ma Y, Wang Z, Fan X and Shan Z: Up-Regulation of miR-26a-5p Inhibits E2F7 to regulate the progression of renal carcinoma cells. *Cancer Manag Res* 12: 11723-11733, 2020.
30. Zhang W, Wu Y, Hou B, Wang Y, Deng D, Fu Z and Xu Z: A SOX9-AS1/miR-5590-3p/SOX9 positive feedback loop drives tumor growth and metastasis in hepatocellular carcinoma through the Wnt/ β -catenin pathway. *Mol Oncol* 13: 2194-2210, 2019.
31. Yang Y, Dong MH, Hu HM, Min QH and Xiao L: LncRNA FGD5-AS1/miR-5590-3p axis facilitates the proliferation and metastasis of renal cell carcinoma through ERK/AKT signalling. *Eur Rev Med Pharmacol Sci* 24: 8756-8766, 2020.
32. Du Y, Lu S, Ge J, Long D, Wen C, Tan S, Chen L and Zhou W: ROCK2 disturbs MKP1 expression to promote invasion and metastasis in hepatocellular carcinoma. *Am J Cancer Res* 10: 884-896, 2020.
33. Deng X, Yi X, Huang D, Liu P, Chen L, Du Y and Hao L: ROCK2 mediates osteosarcoma progression and TRAIL resistance by modulating O-GlcNAc transferase degradation. *Am J Cancer Res* 10: 781-798, 2020.
34. Deng B, Deng J, Yi X, Zou Y and Li C: ROCK2 promotes osteosarcoma growth and glycolysis by up-regulating HKII via Phospho-PI3K/AKT signalling. *Cancer Manag Res* 13: 449-462, 2021.
35. Luo J, Lou Z and Zheng J: Targeted regulation by ROCK2 on bladder carcinoma via Wnt signaling under hypoxia. *Cancer Biomark* 24: 109-116, 2019.
36. Qiu Y, Yuan R, Zhang S, Chen L, Huang D, Hao H and Shao J: Rock2 stabilizes β -catenin to promote tumor invasion and metastasis in colorectal cancer. *Biochem Biophys Res Commun* 467: 629-637, 2015.
37. Amin MB, Edge S, Greene F, Byrd DR, Brookland RK, Washington MK, Gershenwald JE, Compton CC, Hess KR, Sullivan DC, *et al* (eds.). *AJCC Cancer Staging Manual*, 8th edition, Springer, Berlin, Germany, pp 79-81, 2017.



This work is licensed under a Creative Commons Attribution-NonCommercial-NoDerivatives 4.0 International (CC BY-NC-ND 4.0) License.